Supporting Information for:

Strongly Phosphorescent Transition Metal π Complexes of Boron-Boron Triple Bonds

Holger Braunschweig,*[,†,‡] Theresa Dellermann,[†,‡] Rian D. Dewhurst,[†,‡] Benjamin Hupp,[†] Thomas Kramer,[†] James D. Mattock,[§] Jan Mies,[†] Ashwini K. Phukan,[¶] Andreas Steffen,*[,†] Alfredo Vargas[§]

[†] *Institute for Inorganic Chemistry, Julius-Maximilians-Universität Würzburg, Am Hubland, 97074 Würzburg, Germany*

[‡] *Institute for Sustainable Chemistry & Catalysis with Boron, Julius-Maximilians-Universität Würzburg, Am Hubland, 97074 Würzburg, Germany*

[§] *Department of Chemistry, School of Life Sciences, University of Sussex, Brighton BN1 9QJ, Sussex, UK*

[¶] *Department of Chemical Sciences, Tezpur University Napaam 784028 Assam, India*

Materials and Methods

All reactions, unless otherwise noted, were carried out either in an argon-filled glovebox or with rigorous Schlenk techniques. The solvents were dried by storage over, and distillation from, potassium benzophenone (THF), Na/K alloy (pentane) or sodium (benzene) under an argon atmosphere and stored under argon over activated 4 Å molecular sieves. Deuterated benzene was purchased from Sigma Aldrich, degassed by three freeze-pump-thaw cycles and dried over molecular sieves. B_2IDip_2 (**1**) was prepared as previously described.[1] The complex [$Cu(C_2SiMe_3)$] was prepared according to a modified literature procedure using ethynyltrimethylsilane.[2] All solution NMR spectra were acquired on a Bruker Avance 400 NMR spectrometer (400.130 MHz for ^{1}H, 128.385 MHz for ^{11}B, 100.6 MHz for ^{13}C) or on a Bruker Avance I 500 spectrometer (^{1}H: 500.1 MHz, ^{11}B: 160.5 MHz, ^{13}C: 125.8 MHz, ^{29}Si: 99.4 MHz) ^{1}H NMR and ^{13}C{^{1}H} NMR spectra were referenced to external TMS via residual protons of the solvent (^{1}H) or the solvent itself (^{13}C). ^{11}B{^{1}H} NMR spectra were referenced to external $BF_3{\cdot}OEt_2$ and ^{29}Si to external TMS. Melting points were determined with a Metler Toledo 823e DSC apparatus in sealed ampules with a ramp rate of 10 °C/min. Elemental analyses were performed on an Elementar vario MICRO cube elemental analyzer.

Synthetic Procedures

Synthesis of $[B_2(IDip)_2(CuCl)_3]$ (2). B_2IDip_2 (50 mg, 0.062 mmol) was dissolved in 2 mL benzene, 4 equiv [$CuCl(SMe_2)$] (40 mg, 0.25 mmol) was added, and the mixture was stirred at room temperature for 2 d. The suspension was filtered and the solvent was removed in vacuo. The resulting orange solid was washed with hexane (3 × 2 mL) and recrystallized from a dichloromethane/hexane (2:1) mixture. For **2**: 5.5 mg (0.005 mmol, 8%). ^{1}H NMR (500.1 MHz, C_6D_6, 298 K): δ = 7.42 (t, $^3J_{HH}$ = 7.7 Hz, 4 H, CH_{Aryl}), 7.24 (d, $^3J_{HH}$ = 7.8 Hz, 8 H, CH_{Aryl}), 6.17 (s, 4 H, CH_{NHC}), 3.04 (sept., $^3J_{HH}$ = 6.8 Hz, 8 H, CH_{iPr}), 1.58 (d, $^3J_{HH}$ = 6.6 Hz, 24 H, CH_3), 0.92 (d, $^3J_{HH}$ = 6.8 Hz, 24 H, CH_3) ppm. ^{13}C{^{1}H} NMR (125.7 MHz, C_6D_6, 298 K): δ = 146.3 (*o*-C_{aryl}), 133.6 (*i*-C_{aryl}), 132.8 (*p*-CH_{aryl}), 126.2 (*m*-CH_{aryl}), 125.5 (CH_{NHC}), 29.5 (CH_{iPr}), 26.0 (CH_3), 24.9 (CH_3) ppm (the $C_{carbene}$ resonance could not be observed due to broadening caused by ^{11}B–^{13}C coupling). ^{11}B{^{1}H} NMR (128.4 MHz, C_6D_6, 298 K): δ = –7.3 ppm. Elemental analysis (%) calcd. for $C_{54}H_{74}B_2N_4Cu_3Cl_3$: C 59.08 H 6.79 N 5.10; found C 59.80, H 6.60 N 6.16.

Synthesis of $[B_2(IDip)_2\{Cu(C_2SiMe_3)\}_2]$ (3). B_2IDip_2 (50 mg, 62 μmol) was dissolved in 0.6 mL d_6-benzene and 2 equiv [$Cu(C_2SiMe_3)$] (20.1 mg, 0.12 mmol) were added. After stirring for 2 d the solvent

was evaporated in vacuo, yielding 60 mg (0.055 mmol, 86%) of **2** as a red crystalline solid. ^{1}H NMR (500.1 MHz, C_6D_6, 298 K): δ = 7.38 (t, $^{3}J_{HH}$ = 7.75 Hz, 4 H, CH_{Aryl}), 7.20 (d, $^{3}J_{HH}$ = 7.75 Hz, 8 H, CH_{Aryl}), 6.14 (s, 4 H, CH_{NHC}), 2.94 (sept, $^{3}J_{HH}$ = 6.8 Hz, 8 H, CH_{iPr}), 1.34 (d, $^{3}J_{HH}$ = 6.6 Hz, 24 H, CH_{3iPr}), 1.05 (d, $^{3}J_{HH}$ = 6.75 Hz, 24 H, CH_{3iPr}), 0.45 (s, 18 H, SiMe_3) ppm. ^{13}C{^{1}H} NMR (125.7 MHz, C_6D_6, 298 K): δ = 158.9 (br, $C_{carbene}$), 153.7 (Cu*C*C), 145.9 (*o*-C_{aryl}), 134.6 (*i*-C_{aryl}), 130.9 (p-*C*H$_{Aryl}$), 125.2 (m-*C*H$_{Aryl}$), 123.1 (*C*H$_{NHC}$), 101.6 (CuC*C*), 28.9 (*C*H$_{iPr}$), 25.5 (*C*H$_3$), 24.5 (*C*H$_3$), 2.31 (Si(CH_3)$_3$) ppm. ^{11}B{^{1}H} NMR (128.4 MHz, C_6D_6, 298 K): δ = –1.7 ppm. ^{29}Si{^{1}H} NMR (99.35 MHz, C_6D_6, 298 K): δ = –29.04 ppm. Elemental analysis (%) calcd. for $C_{64}H_{92}B_2N_4Cu_2Si_2$: C 68.49 H 8.26 N 4.99; found C 68.66, H 8.16 N 4.84.

Alternative synthesis of 2 from 3. Complex **3** (20 mg, 18 μmol) was dissolved in C_6D_6 (0.6 mL) in a Young-type NMR tube. To this solution [CuCl(SMe$_2$)] (8.6 mg, 53 μmol) was added and shaken overnight. Monitoring by ^{11}B NMR showed quantitative conversion to **2**.

Synthesis of [B$_2$(IDip)$_2$(CuCl)$_2$] (4). 120 mg (107 μmol) of **3** was dissolved in benzene (5 mL) and cooled in an ice bath to ca. 0 °C. To this solution 17.3 mg (107 μmol) [CuCl(SMe$_2$)] was added and the mixture was warmed to room temperature while stirring. The solvent was removed and the residue was suspended in pentane. The yellow solid was washed three times with pentane (3 mL) and dried in vacuo. Slow evaporation of a saturated benzene solution gave crystals of **4** suitable for X-ray diffraction. Yield: 49 mg (51 μmol, 48%) of a yellow solid. ^{1}H NMR (400.1 MHz, C_6D_6, 298 K): δ = 7.36 (t, $^{3}J_{HH}$ = 7.7 Hz, 4 H, CH_{Aryl}), 7.18 (d, $^{3}J_{HH}$ = 7.5 Hz, 8 H, CH_{Aryl}), 6.18 (s, 4 H, CH_{NHC}), 2.85 (sept, $^{3}J_{HH}$ = 6.7 Hz, 8 H, CH_{iPr}), 1.36 (d, $^{3}J_{HH}$ = 6.7 Hz, 24 H, CH_3), 0.98 (d, $^{3}J_{HH}$ = 6.8 Hz, 24 H, CH_3) ppm. ^{13}C{^{1}H} NMR (100.6 MHz, C_6D_6, 298 K): δ = 146.0 (*o*-C_{Aryl}), 134.4 (*i*-C_q), 131.3 (*p*-*C*H$_{Aryl}$), 125.3 (*m*-*C*H$_{Aryl}$), 123.4 (*C*H$_{NHC}$), 29.1 (*C*H$_{iPr}$), 25.6 (*C*H$_{3iPr}$), 24.5 (*C*H$_{3iPr}$) ppm (the $C_{carbene}$ resonance could not be observed due to broadening caused by ^{11}B–^{13}C coupling). ^{11}B{^{1}H} NMR (128.4 MHz, C_6D_6, 298 K): δ = –0.5 ppm. Elemental analysis (%) calcd. for $C_{54}H_{74}B_2N_4Cu_2Cl_2$: C 65.07 H 7.28 N 5.62; found C 65.02, H 7.91 N 5.18.

NMR Spectra

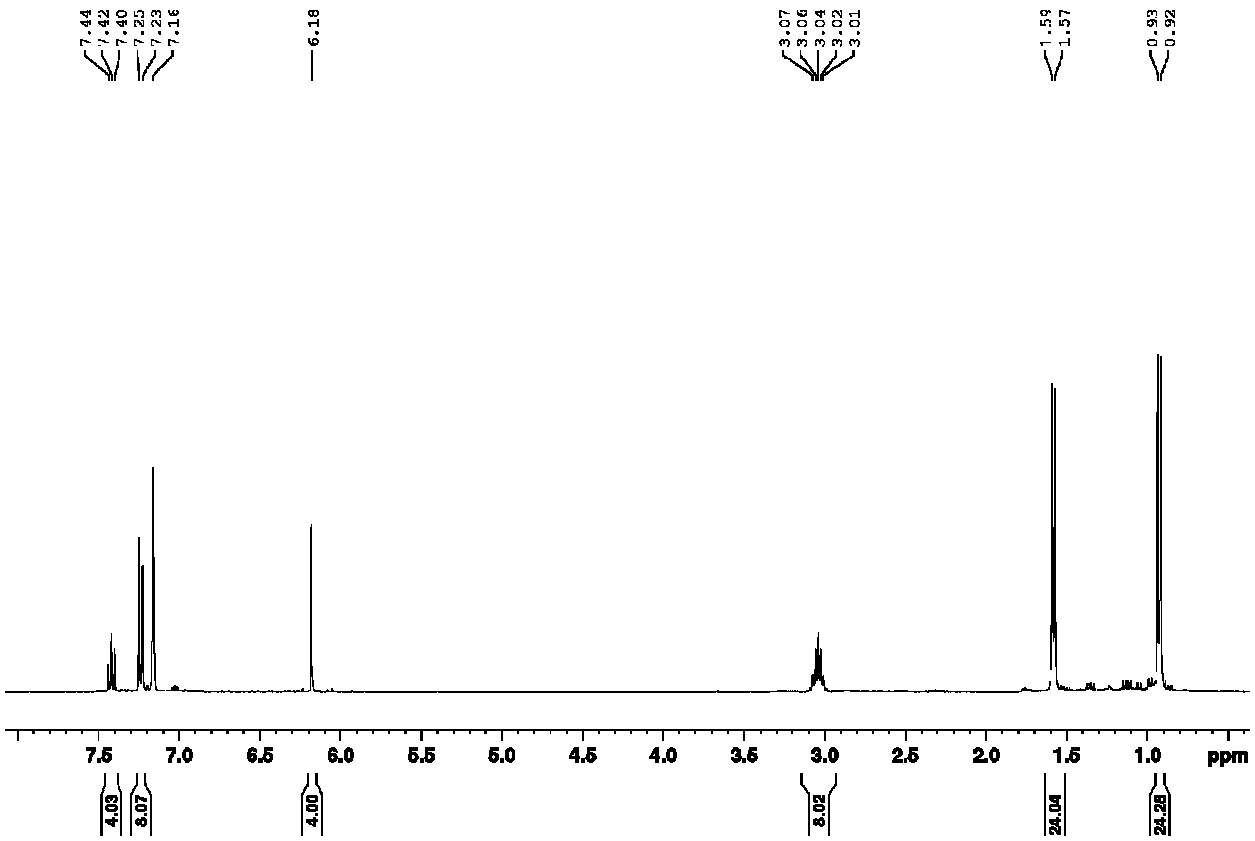

Figure S1. ^{1}H NMR spectrum of compound **2**.

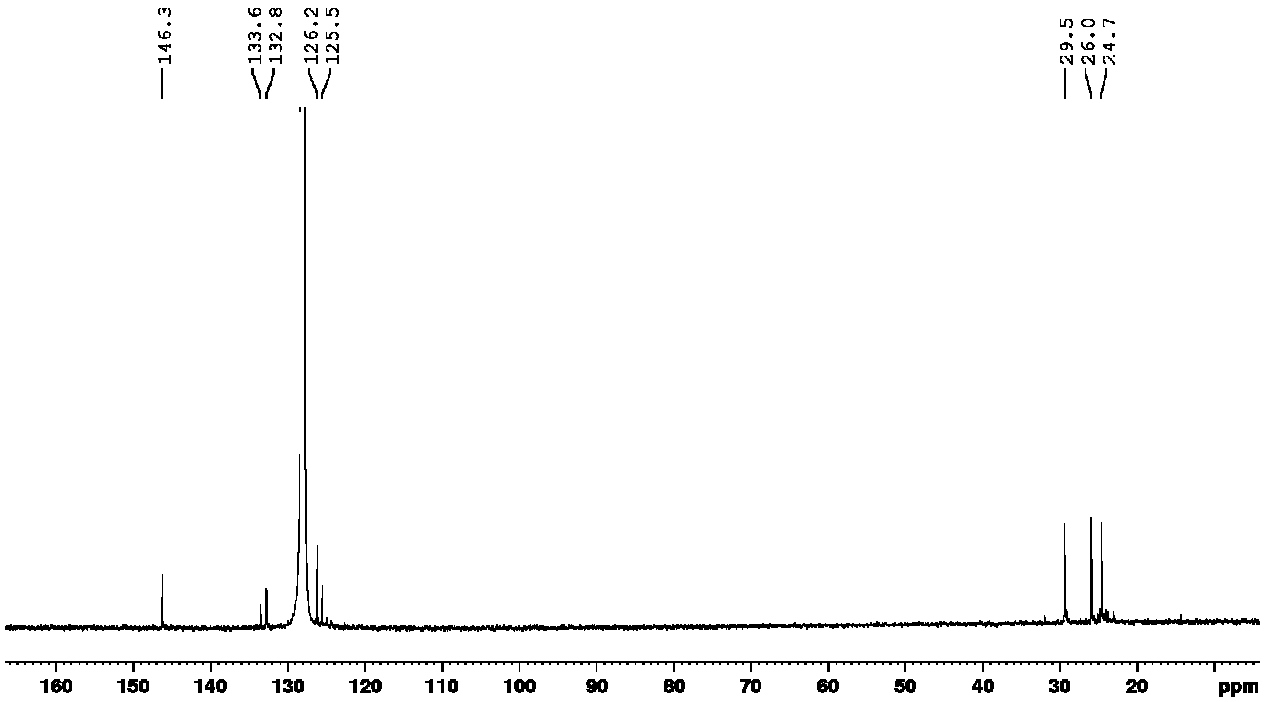

Figure S2. ^{13}C NMR spectrum of compound **2**.

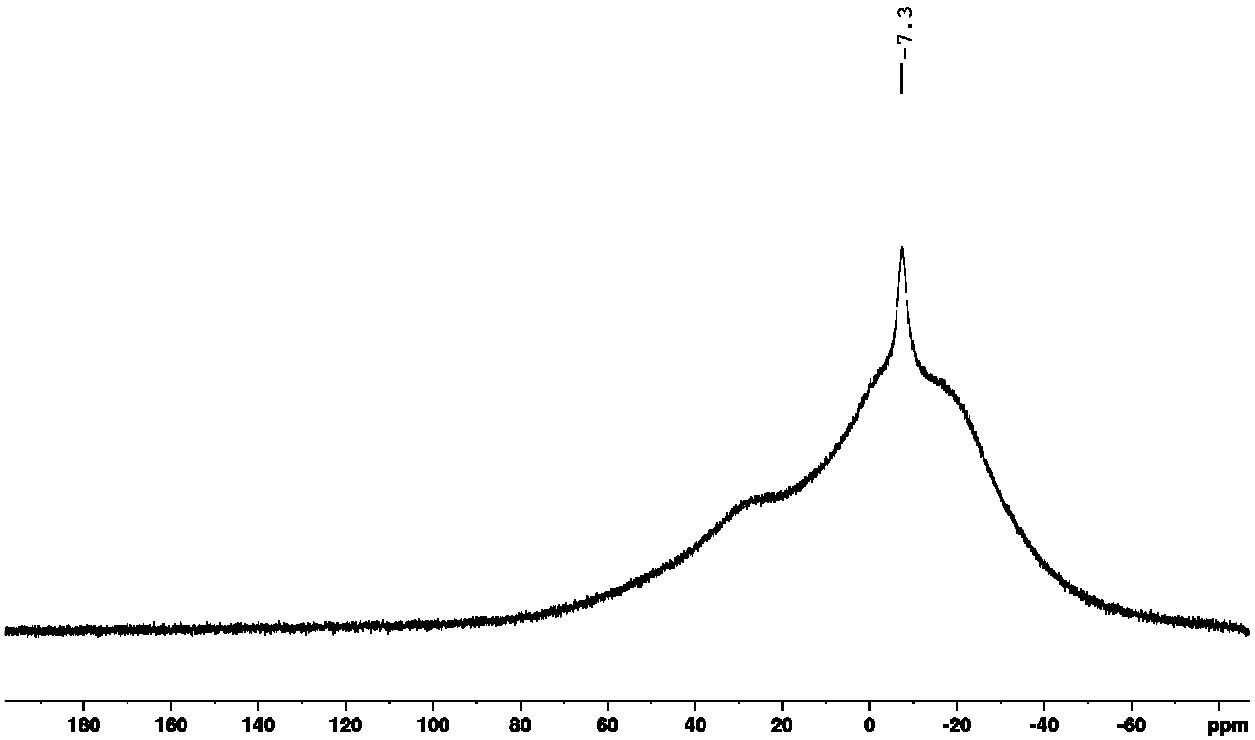

Figure S3. ^{11}B NMR spectrum of compound **2**.

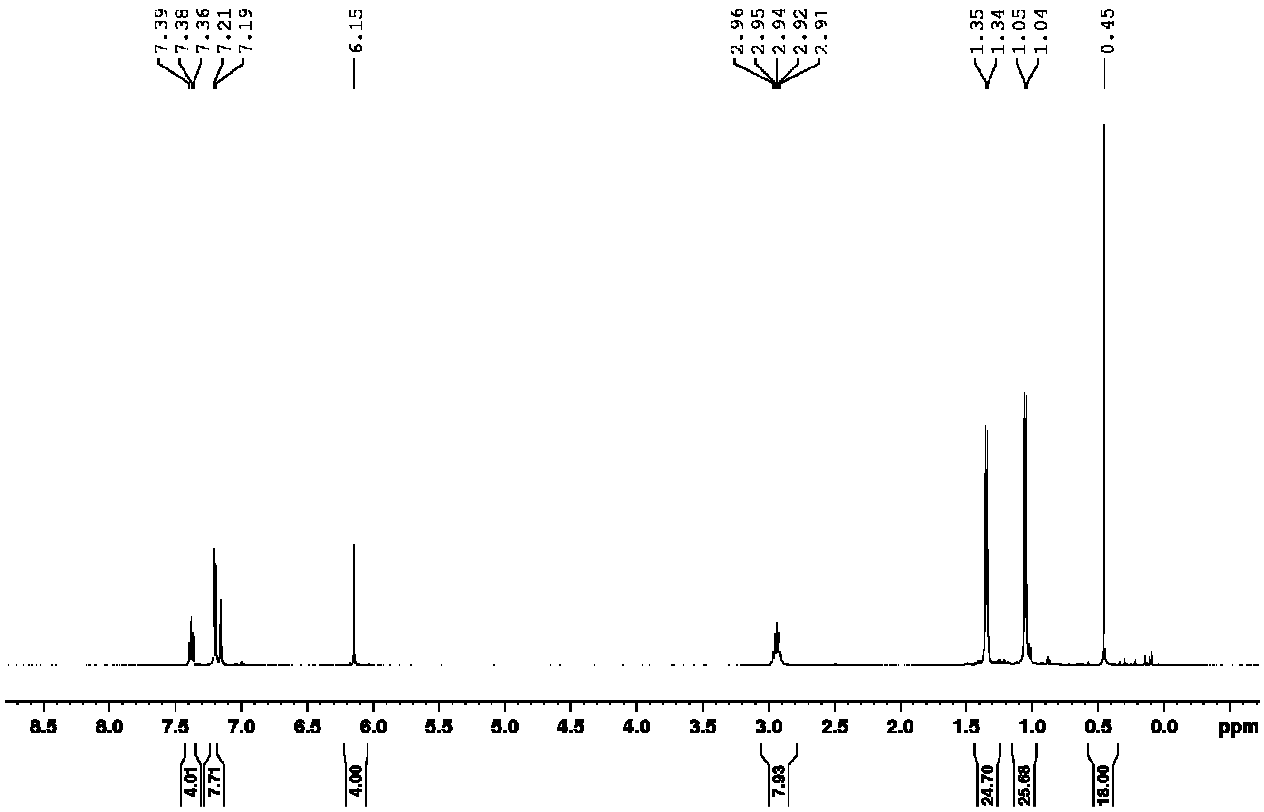

Figure S4. ^{1}H NMR spectrum of compound **3**.

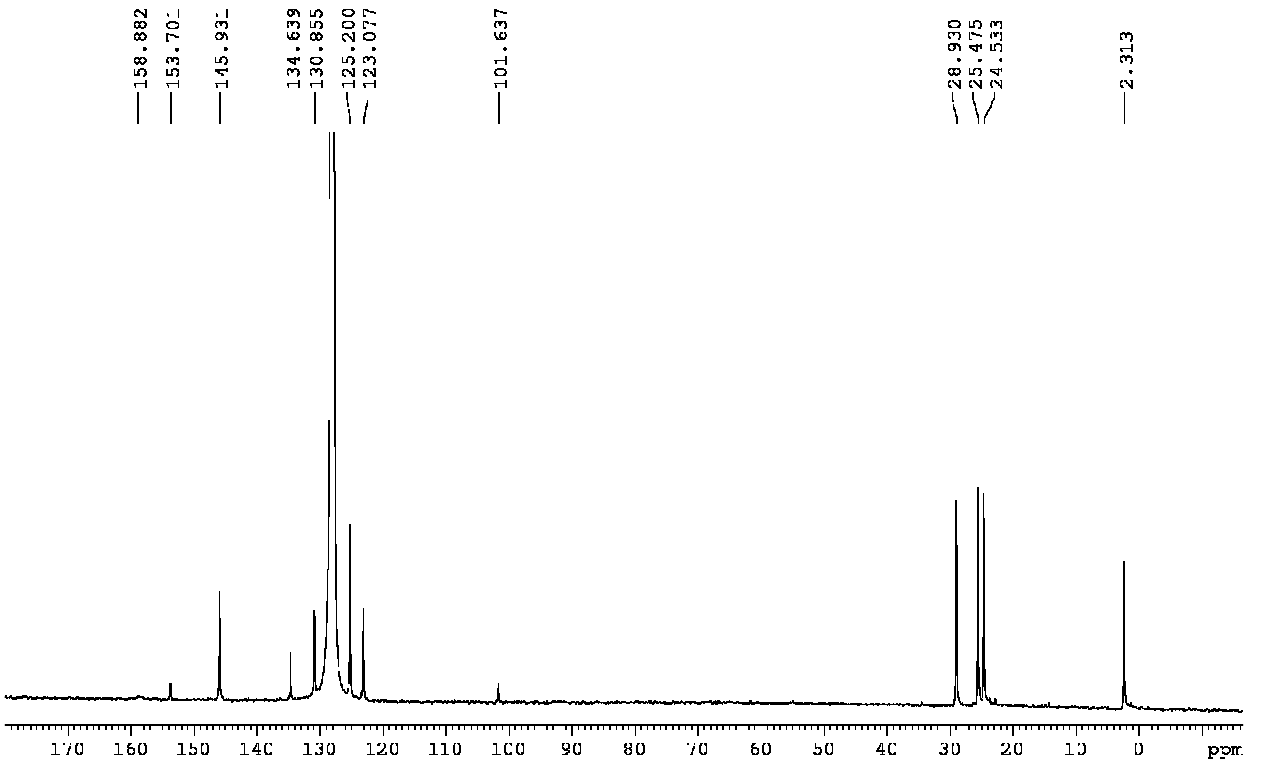

Figure S5. ^{13}C NMR spectrum of compound **3**.

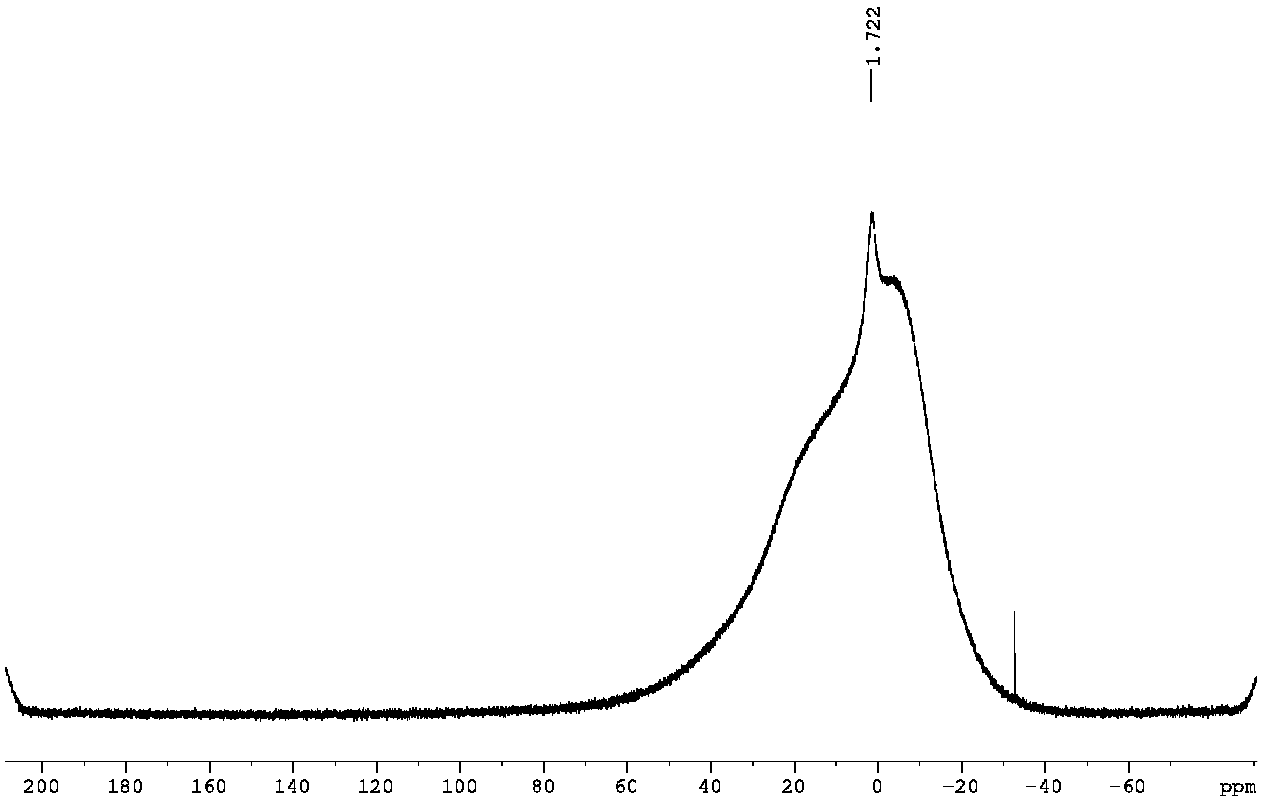

Figure S6. ^{11}B NMR spectrum of compound **3**.

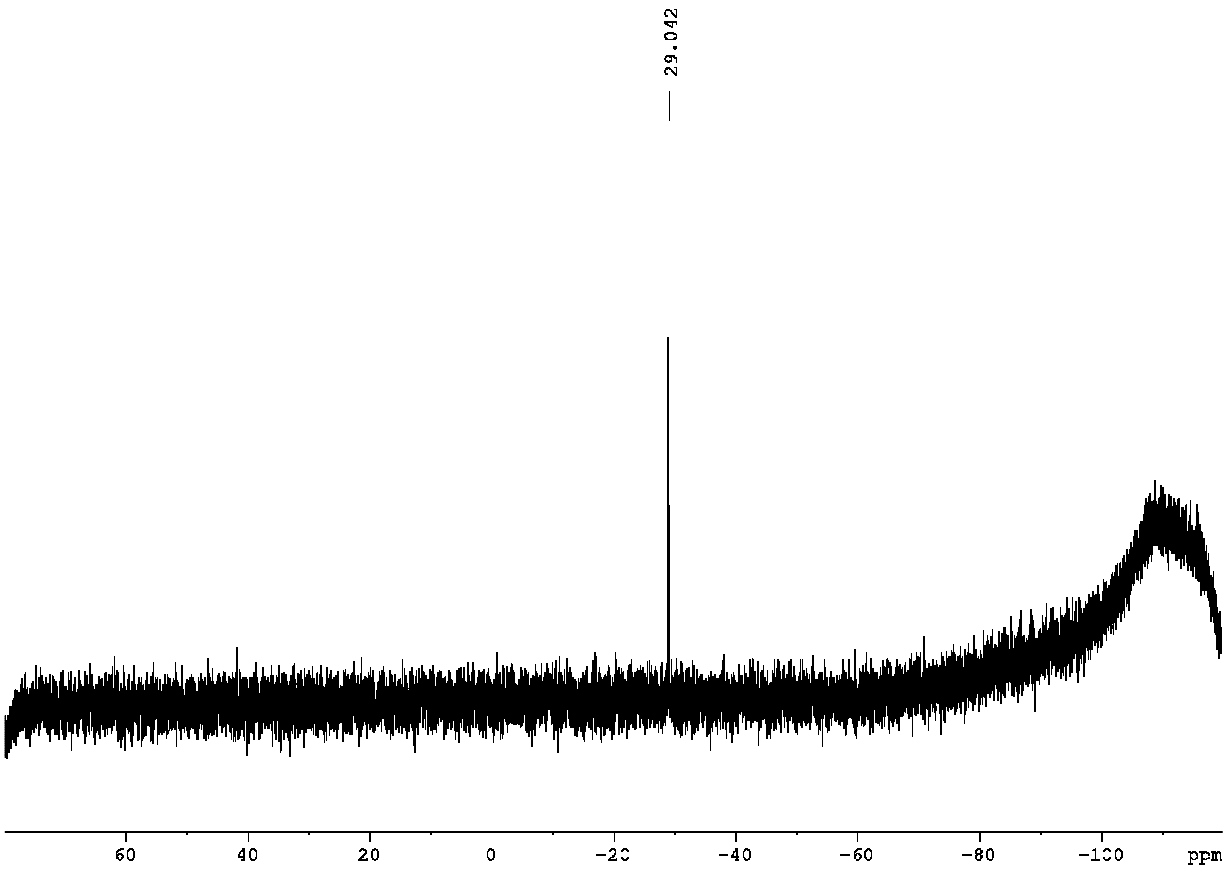

Figure S7. ^{29}Si NMR spectrum of compound **3**.

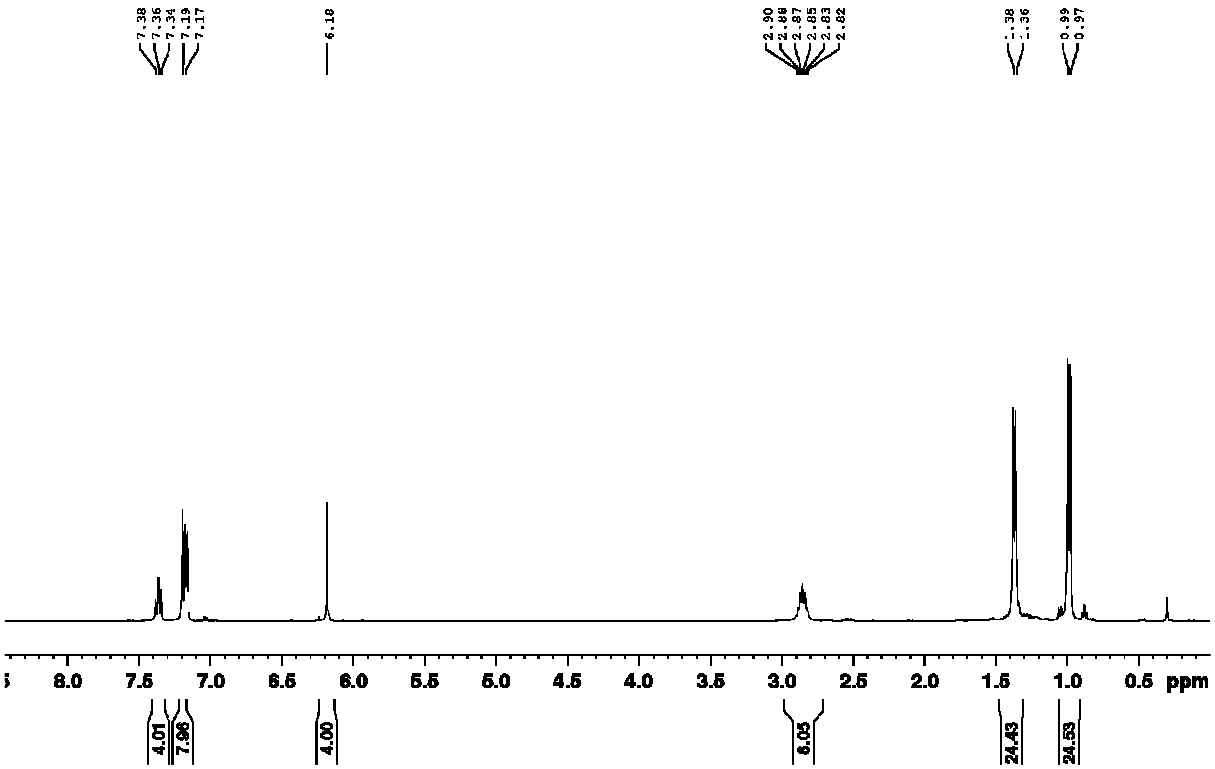

Figure S8. ^{1}H NMR spectrum of compound **4**.

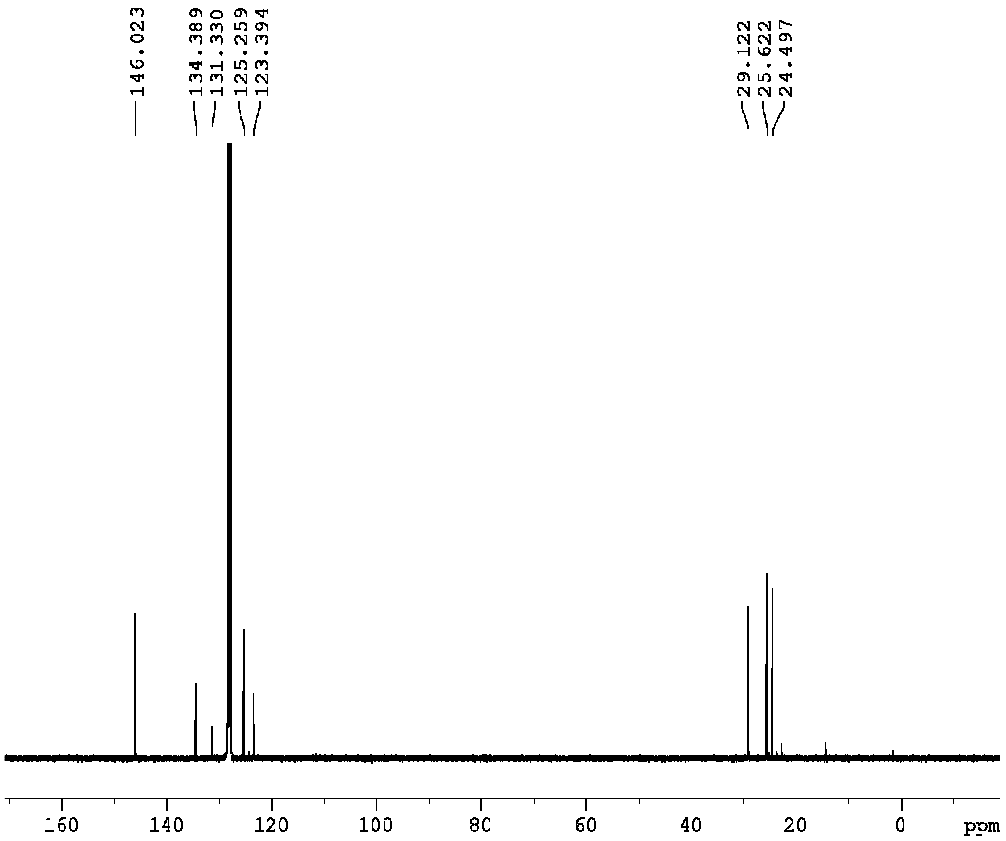

Figure S9. ^{13}C NMR spectrum of compound **4**.

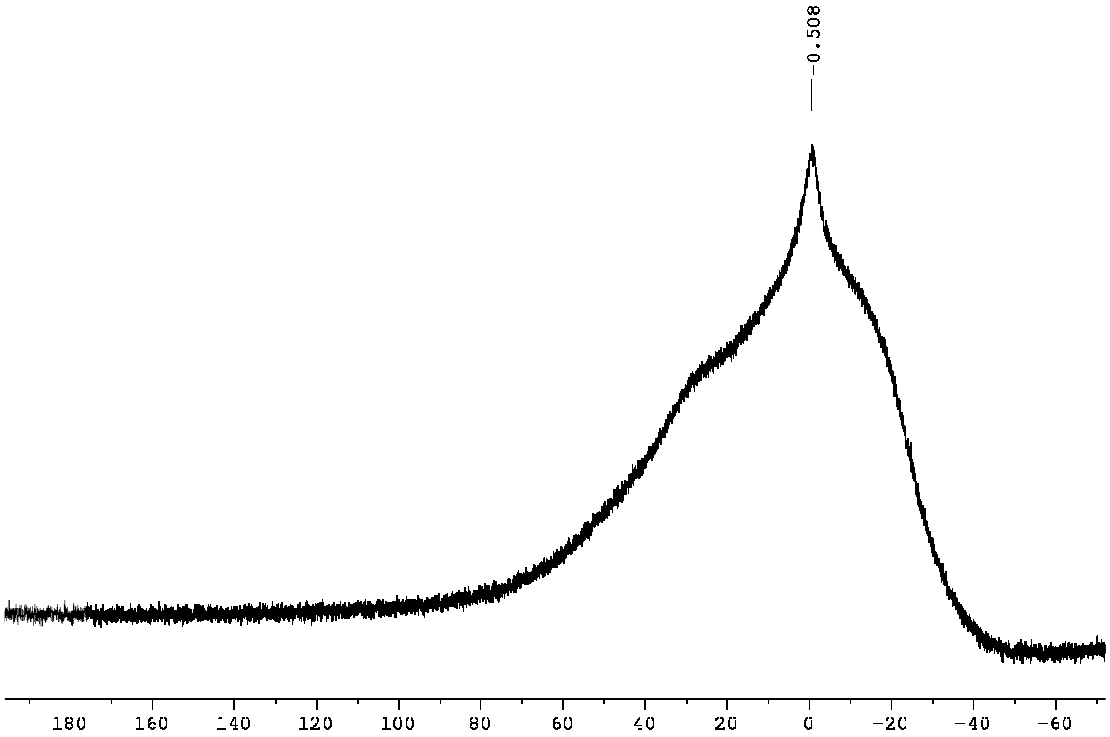

Figure S10. ^{11}B NMR spectrum of compound **4**.

Crystallographic Details

The crystal data of **2** and **3** were collected on a BRUKER X8-APEX II diffractometer with a CCD area detector and multi-layer mirror monochromated $Mo_{K\alpha}$ radiation. The structure was solved using the intrinsic phasing method,[3] refined with the SHELXL program[4] and expanded using Fourier techniques. All non-hydrogen atoms were refined anisotropically. Hydrogen atoms were included in the structure factor calculations. All hydrogen atoms were assigned to idealized geometric positions.

Crystal data for **2**: $C_{54}H_{72}B_2Cl_3Cu_3N_4$, M_r = 1095.74, orange plate, 0.251×0.246×0.051 mm^3, orthorhombic space group *Pccn*, a = 14.408(3) Å, b = 15.791(4) Å, c = 24.221(3) Å, V = 5510.7(19) Å^3, Z = 4, ρ_{calcd} = 1.321 g·cm^{-3}, μ = 1.331 mm^{-1}, $F(000)$ = 2288, T = 296(2) K, R_1 = 0.0422, wR^2 = 0.0840, 5637 independent reflections [2θ≤52.744°] and 307 parameters. The Uii displacement parameters of atoms C91 and C92 of one *iso*propyl group were restrained with the ISOR keyword to approximate isotropic behavior.

Crystal data for **3**: $C_{64}H_{90}B_2Cu_2N_4Si_2$, M_r = 1120.27, red block, 0.23×0.18×0.06 mm^3, monoclinic space group $P2_1/c$, a = 21.5235(9) Å, b = 12.3413(5) Å, c = 25.5747(11) Å, β = 110.5010(10)°, V = 6363.1(5) Å^3, Z = 4, ρ_{calcd} = 1.169 g·cm^{-3}, μ = 0.746 mm^{-1}, $F(000)$ = 2392, T = 296(2) K, R_1 = 0.0351, wR^2 = 0.0793, 12544 independent reflections [2θ≤52.044°] and 689 parameters.

The crystal data of **4** were collected on a BRUKER D8 QUEST diffractometer with a CMOS area detector and multi-layer mirror monochromated $Mo_{K\alpha}$ radiation. The structure was solved using the intrinsic phasing method,[3] refined with the SHELXL program[4] and expanded using Fourier techniques. All non-hydrogen atoms were refined anisotropically. Hydrogen atoms were included in the structure factor calculations. All hydrogen atoms were assigned to idealized geometric positions.

Crystal data for **4**: $C_{60}H_{78}B_2Cl_2Cu_2N_4$, M_r = 1074.86, orange block, 0.21×0.198×0.114 mm^3, monoclinic space group $P2_1/c$, a = 14.580(7) Å, b = 16.059(9) Å, c = 24.981(13) Å, β = 93.26(4)°, V = 5840(5) Å^3, Z = 4, ρ_{calcd} = 1.223 g·cm^{-3}, μ = 0.859 mm^{-1}, $F(000)$ = 2272, T = 100(2) K, R_1 = 0.0816, wR^2 = 0.1136, 11457 independent reflections [2θ≤52.044°] and 647 parameters.

Crystallographic data have been deposited with the Cambridge Crystallographic Data Center as supplementary publication nos. CCDC-1517608 (**2**), -1517609 (**3**) and -1517610 (**4**). These data can be

obtained free of charge from The Cambridge Crystallographic Data Centre *via* www.ccdc.cam.ac.uk/data_request/cif

UV-vis and Emission Spectroscopy

UV-vis spectra were measured on a JASCO V-660 spectrometer in dried and degassed solvents in 1 cm quartz glass cuvettes. Excitation and emission spectra were recorded on an Edinburgh Instruments FLSP920 spectrometer, equipped with a 450 W xenon lamp, double monochromators for the excitation and emission pathways, and photomultipliers (PMT-R928-P and PMT-R5509-42) as detectors. The excitation and emission spectra were fully corrected using the standard corrections supplied by the manufacturer for the spectral power of the excitation source and the sensitivity of the detector.

The luminescence lifetimes were measured either via time-correlated single photon counting (TCSPC) using a 420 nm or 376 nm pulsed ps laser diode (5 mW), or via a multi-channel scaling (MSC) module with a μs flash lamp as excitation source. The emission was collected at right angles to the excitation source with the emission wavelength selected using a double grated monochromator and detected by a R928-P or a R5509-42 PMT. For TCSPC mode, the instrument response function (IRF) was measured using the blank solvent as scattering sample and setting the monochromator at the emission wavelength of the laser diode, giving an IRF of 900 ps at 420 or 376 nm. The resulting intensity decay is a convolution of the luminescence decay with the IRF and iterative reconvolution of the IRF with a decay function and non-linear least squares analysis was used to analyze the convoluted data.

Determination of the absolute quantum yield was performed with an integrating sphere. First, the diffuse reflection of the sample was determined under excitation (λ_{exc} = 420 nm). Second, the emission was measured for this excitation wavelength. Integration over the reflected and emitted photons allows calculation of the absolute quantum yield.

Computational Methods

Geometry optimization was carried out in the gas phase using the Gaussian09 program at the ωB97XB/Def2-SVP (H, B, C, N, Cl, Si), Def2-TZVP (Cu) level[5-7] as well as using the Amsterdam Density Functional (ADF) program[8-10] at the B3LYP*/TZP level.[11-13] The Wiberg bond indexes (WBI)[14] and natural charges were determined in the Natural Bond Orbital (NBO)[15,16] basis. Spin-restricted calculations were performed by constraining the projection of the total electronic spin along a reference axis to zero. Frequency calculations were conducted to determine if each stationary point corresponds to a minimum.[17-19] The nature of the bonding of the copper moieties to the diboryne was described using the energy decomposition analysis[20-22] (EDA) (also known as the "fragment approach") according to the methods of Morokuma, Ziegler and Rauk. Using the EDA scheme, the energy E_{int} associated with the interaction between the fragments L-Cu and R-B-B-R can be divided into three components: $E_{int} = E_{elstat}+E_{Pauli}+E_{orb}$; the first term, E_{elstat}, corresponds to the classical electrostatic interaction between the unperturbed charge distributions of the fragments (the overall density being the superposition of the fragment densities). The second term, E_{Pauli}, expresses the energy change that arises upon going from the simple superposition of the fragment densities to the wavefunction that obeys the Pauli principle through antisymmetrization and normalization of the product of the fragment wavefunctions. In the last term, E_{orb}, the energy that originates from the contributions from stabilizing orbital interactions (electron pair bonding, charge transfer, polarization) is given. To further describe the nature of the bonds of interest, we employed techniques based on the so-called ETS-NOCV formalism,[23] hence to describe the charge flux process taking place upon adduct formation, the natural orbitals for chemical valence (NOCV) description was used. It is based on the NOCV wavefunction as an eigenvector of the deformation density matrix in the basis of fragment orbitals. A useful piece of qualitative data is the sign of $\Delta\rho$, negative for an outflow of charge and positive for an inflow of charge, in going from the constituent fragments to the whole system. In order to optimize the geometry of the orthogonal conformation of **4'** the Cu-B-B-Cu dihedral angle was constrained to 90º. The ADF Graphical User Interface (ADF-GUI – a part of the ADF package) was used for visualisation purposes.

At the at wB97XD/Def2-SVP, Def2-TZVP level, in agreement with experiment, the calculations also reproduce the weakening and strengthening of the B≡B units and B–C bonds, respectively, as the degree of metalation increases from **3** and **4** to **2** (Table S1). The B–Cu bonds are not very strong, as evident from the computed Wiberg Bond Index values (0.24 – 0.27). The computations yield three distinct BB-centered occupied molecular orbitals corresponding to one σ and two π bonds between the boron atoms. Similar to the diborene-CuCl complex **III**, the computed frontier orbitals of **2**–**4** indicated presence of a BB-centered HOMO with a slight distortion towards one copper unit (Figure S11) which accounts for the weakening of

the B–B triple bond. NBO calculations show a significant amount of residual negative and positive charges at the boron (–0.339 to –0.437) and copper (+0.478 to +0.507) atoms. This is in contrast to the computed charges at the boron (–0.056) and copper (0.464) centers in **III**, implying stronger electrostatic interaction between B and Cu in **2-4** than that in **III**. This is also evident from the significantly smaller electrostatic contribution in **III** compared to that in **2** (E_{el} = –145 and –432 kcal mol^{-1} in **III** and **2** respectively, *vide infra*).[24] Further, for the sake of comparison, we also optimized a hypothetical copper-alkyne complex (Figure S12). Interestingly, the computed natural charges indicate strong electrostatic interaction between carbon (–0.509) and copper (–0.515) similar to that in **2**–**4**.

Table S1. wB97XD/Def2-SVP, Def2-TZVP (only for Cu) calculated distances between – (i) boron atoms (r_{B-B}), (ii) the boron and copper (r_{B-Cu}) atoms, (iii) boron and the central carbon atom of the NHC units (r_{B-Cc}) and natural charges at the boron (q_B) and copper (q_{Cu}) atoms, respectively. The Wiberg Bond Index (WBI) values are given in parentheses while the experimentally observed values are given in italics.

Molecule	$\mathbf{r_{B-B}}$ **(Å)**	$\mathbf{r_{B-Cu}}$ **(Å)**	$\mathbf{r_{B-Cc}}$ **(Å)**	$\mathbf{q_B}$	$\mathbf{q_{Cu}}$
1	1.470	-	1.488	–0.152	**-**
	(2.016)		(1.168)		
	1.449		*1.487, 1.495*		
2	1.519	2.114 (av.)	1.564	–0.437	0.494 (av.)
	(1.987)	(0.243 av.)	(0.934)		
	1.526	*2.077 (av.)*	*1.562*		
3	1.475	2.118 (av.)	1.536	–0.339	0.478
	(2.035)	(0.271)	(0.966)		
	1.478	*2.087*	*1.531, 1.535*		
4	1.485	2.108	1.542	–0.388	0.507
	(2.107)	(0.250)	(0.965)		
	1.486	*2.079 (av.)*	*1.545, 1.547*		

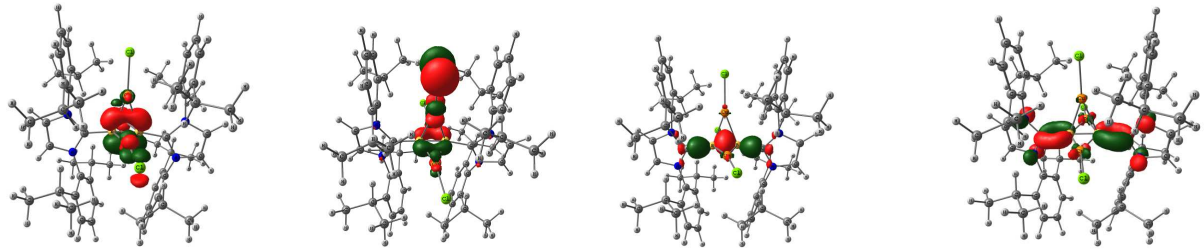

HOMO (–7.3 eV) HOMO-1 (–7.6 eV) HOMO-91 (–13.9 eV) LUMO (–0.6 eV)

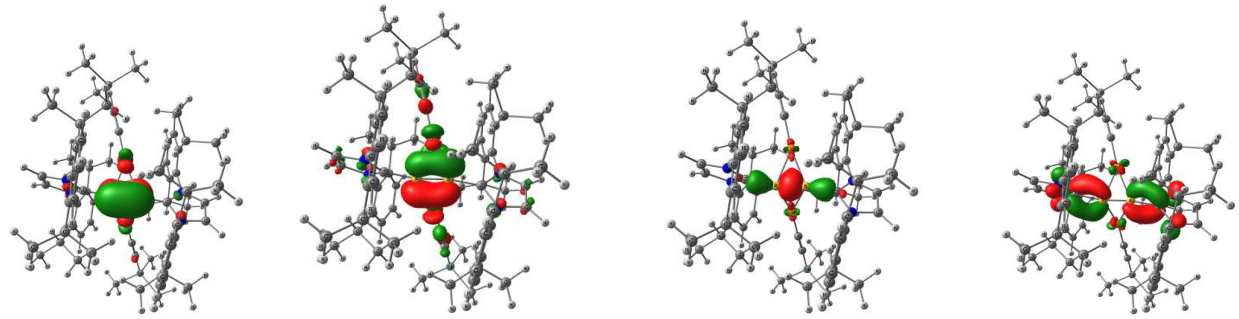

HOMO (–6.4 eV) HOMO–1 (–7.0 eV) HOMO–89 (–13.0 eV) LUMO (0.16 eV)

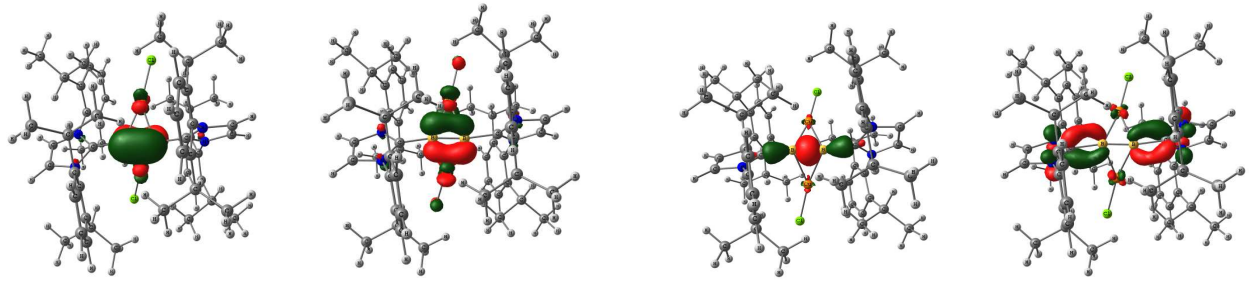

HOMO (–6.5 eV) HOMO–1 (–7.0 eV) HOMO–73 (–13.0 eV) LUMO (0.2 eV)

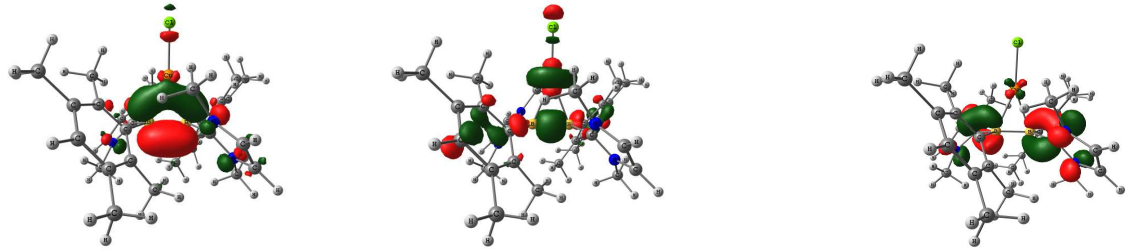

HOMO (–6.0 eV) HOMO–1 (–7.3 eV) LUMO (0.8 eV)

Figure S11. Important molecular orbitals of **2** (first row), **3** (second row), **4** (third row) and **III** (fourth row) optimized at the ωB97XB/Def2-SVP, Def2-TZVP level of theory.

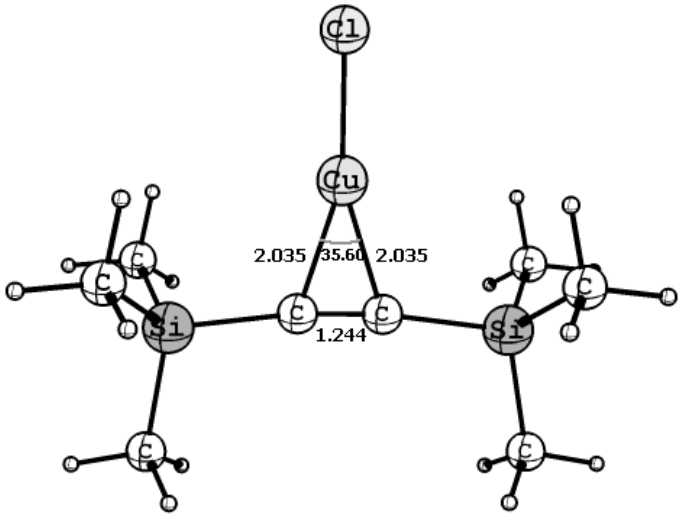

Figure S12. ωB97XB/Def2-SVP, Def2-TZVP optimized geometry of a hypothetical copper-alkyne complex.

References

(1) Braunschweig, H.; Dewhurst, R. D.; Hammond, K.; Mies, J.; Radacki, K.; Vargas, A. *Science* **2012**, *336*, 1420-1422.

(2) Jouvin, K.; Heimburger, J.; Evano, G. *Chem. Sci.* **2012**, *3*, 756-760.

(3) Sheldrick, G. *Acta Cryst.* **2015**, *A71*, 3–8.

(4) Sheldrick, G. *Acta Cryst.* **2008**, *A64*, 112–122.

(5) Frisch, M. J.; Trucks, G. W.; Schlegel, H. B.; Scuseria, G. E.; Robb, M. A.; Cheeseman, J. R.; Scalmani, G.; Barone, V.; Mennucci, B.; Petersson, G. A.; Nakatsuji, H.; Caricato, M.; Li, X.; Hratchian, H. P.; Izmaylov, A. F.; Bloino, J.; Zheng, G.; Sonnenberg, J. L.; Hada, M.; Ehara, M.; Toyota, K.; Fukuda, R.; Hasegawa, J.; Ishida, M.; Nakajima, T.; Honda, Y.; Kitao, O.; Nakai, H.; Vreven, T.; Montgomery, J. A.; Jr.; Peralta, J. E.; Ogliaro, F.; Bearpark, M.; Heyd, J. J.; Brothers, E.; Kudin, K. N.; Staroverov, V. N.; Keith, T.; Kobayashi, R.; Normand, J.; Raghavachari, K.; Rendell, A.; Burant, J. C.; Iyengar, S. S.; Tomasi, J.; Cossi, M.; Rega, N.; Millam, J. M.; Klene, M.; Knox, J. E.; Cross, J. B.; Bakken, V.; Adamo, C.; Jaramillo, J.; Gomperts, R.; Stratmann, R. E.; Yazyev, O.; Austin, A. J.; Cammi, R.; Pomelli, C.; Ochterski, J. W.; Martin, R. L.; Morokuma, K.; Zakrzewski, V. G.; Voth, G. A.; Salvador, P.; Dannenberg, J. J.; Dapprich, S.; Daniels, A. D.; Farkas, O.; Foresman, J. B.; Ortiz, J. V.; Cioslowski, J.; Fox, D. J. Gaussian 09, Revision D.01. Gaussian, Inc., Wallingford, CT, 2013.

(6) Chai, J.-D.; Head-Gordon, M. *Phys. Chem. Chem. Phys.* **2008**, *10*, 6615-6620.

(7) (a) Zhao, Y.; Truhlar, D. G. *Theor. Chem. Acc.* **2008**, *120*, 215-241; (b) Weigend, F.; Alhrichs, R. *Phys. Chem. Chem. Phys.* **2005**, *7*, 3297-3305; (c) Weigend, F. *Phys. Chem. Chem. Phys.* **2006**, *8*, 1057-1065.

(8) te Velde, G.; Bickelhaupt, F. M.; Baerends, E. J.; Fonseca Guerra, C.; van Gisbergen, S. J. A.; Snijders, J. G.; Ziegler, T. *J. Comput. Chem.* **2001**, *22*, 931-367.

(9) Fonseca Guerra, C.; Snijders, J. G.; te Velde, G.; Baerends, E. J. *Theor. Chem. Acc.* **1993**, *99*, 391-403.

(10) ADF2016, SCM, Theoretical Chemistry, Vrije Universiteit, Amsterdam, The Netherlands, http://www.scm.com.

(11) Reiher, M.; Salomon, O.; Hess, B. A. *Theor. Chem. Acc.* **2001**, *107*, 48-55.

(12) van Lenthe, E.; Baerends, E. J. *J. Comput. Chem.* **2003**, *24*, 1142-1156.

(13) Autschbach, J. *Chem. Phys. Chem.* **2009**, *10*, 2274-2283.

(14) Wiberg, K. *Tetrahedron* **1968**, *24*, 1083-1096.

(15) Weinhold, F.; Landis, C. R. Valency and Bonding: A Natural Bond Orbital Donor-Acceptor Perspective. Cambridge University Press, Cambridge, U.K., 2005.

(16) Reed, A. E.; Curtiss, L. A.; Weinhold, F. *Chem. Rev.* **1988**, *88*, 899-926.

(17) Bérces, A.; Dickson, R. M.; Fan, L.; Jacobsen, H.; Swerhone, D.; Ziegler, T. *Comput. Phys. Commun.* **1997**, *100*, 247-262.

(18) Jacobsen, H.; Bérces, A.; Swerhone, D.; Ziegler, T. *Comput. Phys. Commun.* **1997**, *100*, 263-276.

(19) Wolff, S. K. *Int. J. Quantum. Chem.* **2005**, *104*, 645-659.

(20) Ziegler, T.; Rauk, A. *Inorg. Chem.* **1979**, *18*, 1558-1565.

(21) Ziegler, T.; Rauk, A. *Inorg. Chem.* **1979**, *18*, 1755-1759.

(22) Bickelhaupt, F. M.; Baerends, E. J. in: *Reviews in Computational Chemistry*; Lipkowitz; K. B.; Boyd, D. B. Eds.; Wiley, New York, 2000, Vol. 15, pp 1-86.

(23) Mitoraj, M.; Michalak, A.; Ziegler, T. *J. Chem. Theory Comput.* **2009**, *5*, 962-975.

(24) Bissinger, P.; Steffen, A.; Vargas, A.; Dewhurst, R. D.; Damme, A.; Braunschweig, H. *Angew. Chem., Int. Ed.* **2015**, *54*, 4362-4366.